Journal of Thermal Analysis, Vol. 35 (1989) 1651–1667

THERMOGRAVIMETRIC STUDY OF THE $C + SiO_2$ REACTION*

*J. J. Biernacki*** and *G. P. Wotzak****

BRITISH PETROLEUM AMERICA, RESEARCH AND DEVELOPMENT, CLEVELAND, OHIO
FENN COLLEGE OF ENGINEERING, CLEVELAND STATE UNIVERSITY, CLEVELAND, OHIO, U.S.A.

(Received November 5, 1988; in revised form January 19, 1989)

The kinetics of the reaction of one-to-one molar mixtures of crystalline silica and carbon powder were studied using thermogravimetric analysis. The resulting kinetic data was evaluated using simple kinetic and mass transport models. A two-stage reaction mechanism consisting of three stoichiometric reactions can adequately be used to describe the global reaction phenomena. Both the first and second stages of reaction were found to be influenced by diffusion mass transfer within the reacting bed of solids.

Although the reaction between silica and carbon has been studied for many years, the basic reaction mechanism is yet to be fully described and understood. While the kinetics of this reaction have been studied by many investigators, some aspects of the C/SiO_2 interaction have not been described since the diverse nature of carbon and silica add to the difficulty in isolating the intrinsic kinetic behaviour.

Recently, Biernacki [1] has put forth a reaction path mechanism in which the three interrelated reaction stoichiometries occur during the SiO_2/C reaction between 1200 and 1650°. In a study designed to investigate the stoichiometry of the one-to-one molar reaction of SiO_2 and C the following reaction path mechanism was established.

$$SiO_2(s) + C(s) \rightarrow SiO_2(g) + CO(g) \quad (1)$$

$$SiO_2(g) + 2\,C(s) \rightarrow SiC(s) + CO(g) \quad (2)$$

$$2\,SiO_2(s) + SiC(s) \rightarrow 3\,SiO(g) + CO(g) \quad (3)$$

The forms of the kinetic rate expressions for these reactions are, however, unknown. The literature suggests that the global C/SiO_2 reaction is zero order for

* This paper is based on the doctoral dissertation of the senior author.

** Present address: Carborundum, Niagara Falls, NY 14302 U.S.A.

*** Present address: Fenn college of Engineering, Cleveland State University, 1983 E. 24th St., Stilwell Hall 104, Cleveland, Ohio 44115 U.S.A.

John Wiley & Sons, Limited, Chichester
Akadémiai Kiadó, Budapest

low extent of reaction [2, 3, 4]. The zero order result is most likely an empirical coincidence in these and other studies. Klinger et al. [2], however, explained the zero order dependence as the result of a reaction mechanism which proceeds via the decomposition/evaporation of silica with subsequent reaction with carbon and control by Langmuir–Knudsen conditions. Lee and Cutler [3] also suggested that the SiO_2/C reaction precedes via the decomposition of SiO_2 and subsequent reaction with C by demonstrating that the rate of reaction increases as the surface area of SiO_2 increases. A wide variety of SiO_2 and C sources have been studied. Henderson and Tant [5] applied an empirical model to evaluate the high temperature decomposition of polymer char and silica glass fibers and found good results for extents of reaction from zero to one. These earlier studies on the SiO_2/C reaction, however, have not assessed the effect of transport conditions on the rate of reaction.

The effect of CO over-pressure has been presented in the literature and is of particular interest since CO is a reaction product. Again the resulting expressions are empirical in nature and address the observed effect on the global reaction rate only. Klinger et al. [2] suggested a rate expression having an inverse 1/3 P_{CO} dependence for SiC formation:

$$dSiC/dt \propto 1/P_{CO}^{1/3} \tag{4}$$

This expression, however, is mathematically inconsistent for CO pressures approaching zero. Klinger et al. also reported autocatalytic behaviour proportional to the 1/3 power of the CO pressure:

$$dn_{co}/dt \propto P_{co}^{1/3} \tag{5}$$

where n_{co} is the moles of CO formed. This result was found to hold only at high temperatures and for long reaction times and was attributed to activation of the sample upon a SiO_2 phase change.

In order to better describe the C–SiO_2 reaction, this study focuses on the rate controlling processes during the reaction of crystalline SiO_2 powder and carbon powder.

Experimental

Quartz 240 mesh floated silica [6] was used as the SiO_2 reagent and pyrolyzed methane carbon powder [7] was used as the carbon source. The silica had a nominal particle size of 40 microns while the carvon was on the order of one micron. Both reagents were used as received. The carbon source contained 99.1 weight percent carbon with the remainder being primarily hydrogen (0.39%), nitrogen (0.28%), Si

(330 ppm), Al (250 ppm), Ca (170 ppm), Na (120 ppm), and other elements in trace amounts (< 60 ppm each, 846 ppm total), with a BET surface area of 10.2 meters squared per gram. The silica was at least 98.2 percent SiO_2 with quantified impurity including hydrogen (1500 ppm), nitrogen (1500 ppm), Fe (600 ppm), carbon (400 ppm), Al (370 ppm), Ti (190 ppm), Ba (15 ppm), and Mg (8.5 ppm). More detailed analytical information can be found elsewhere [1].

One-to-one molar mixtures of C and SiO_2 were prepared in a single large lot by placing the appropriate amounts of C and SiO_2 in a container and shaking vigorously until a uniform mixture was achieved. Portions of the mother lot were used for each experiment.

The experimental apparatus consisted of a Netzsch simultaneous thermal analyzer model 409/STA. A detailed description of the apparatus and the operating procedures can be found elsewhere [1].

The use of thermogravimetric analysis can often confound the data by imposing transport or other limitations on the reacting system. When TGA is used to study reaction kinetics it is prudent to design experiments in such a way that transport effects can be avoided or at least be well characterized and identified. Many techniques for analyzing TGA data are available from Kissinger [8], Freeman and Carroll [9], Coats and Redfern [10], Friedman [11], Ozawa [12], Sharp and Wentworth [13], Flynn [14] and Elder [15]. Such analyses are powerful tools but can be misleading in the absence of the knowledge of which phenomenological processes influence the rate of reaction. Although many of the techniques are designed to identify rate controlling mechanisms by mathematical analysis, it is typically not clear from a single experiment or poorly designed series of experiments which of the given phenomena influence the reaction rate. The rate controlling process can be established experimentally by searching for limiting behavior, i.e. diffusion limited behavior, kinetic controlled behavior, etc., rather than by applying a mathematical model which is often forced to fit the observed data. The models approach can be useful, however, assuming that good results are either supported by evidence which identifies the rate controlling processes or are interpreted as possibly being an empirical coincidence.

Blank runs or control experiments were performed where—in the buoyance effects and reactivity of the pure reagents were characterized. Buoyance was found to simulate a 1 mg increase in weight (1% deviation in 100 mg, 0.1% deviation in 1000 mg, etc.) over a temperature range from 20° to 1000°. Above 1000° buoyance effects were negligibly small. Pure reagent reactivity was also found to be negligibly small in comparison to the weight changes observed during reaction.

Two series of experiments were designed. The first was a single series of three experiments used to screen the effect of initial sample weight on the resulting TGA kinetics. For these experiments samples weighing nominally W_0, $2W_0$, and $3W_0$,

where W_0 equals the initial sample weight for the first experiment, were reacted under identical conditions of heating rate (10 deg/min) and gas flowrate. The second series of experiments was designed so that the experimental variables were manipulated such that the independent effects of heat and mass transfer, and CO over-pressure could be identified.

In order to test the influence of transport effects combined with the effects of CO over-pressure, it was necessary to:

1. hold the sample mass and the geometry of the sample bed constant,
2. vary the diffusion path through the powder bed,
3. vary the thermal mass of the sample,
4. vary the CO over-pressure,
5. vary the gas phase diffusion path length.

An experimental design was developed with the physical situation given in Fig. 1. The reactant bed had constant initial bed thickness and constant cross-sectional area with a resulting constant initial mass. Two inert layers of SiO_2 were used to vary the diffusion path length through the solid bed and to control the thermal mass of the system. The inert layers were placed above and below the reactant bed. The top inert layer was used to control the intra-bed diffusion path length while the bottom inert layer was used to control the total thermal mass of the system. The gas phase diffusion path length through the gaseous layer above the bed was varied by

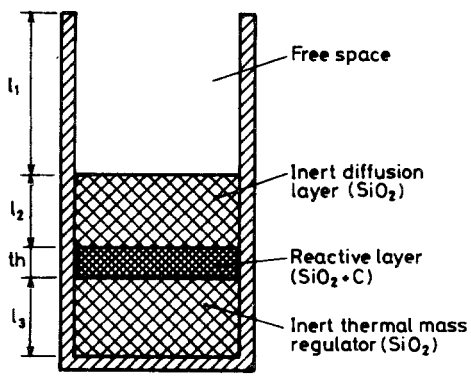

l_1 = Free space above surface of diffusion layer and top of crucible,

l_2 = Thickness of inert diffusion layer,

l_3 = Thickness of inert layer used to control the total thermal mass of the system,

th = Thickness of the reactive sample layer.

Fig. 1 Experimental design used to control the factors which influence the observed rate of reaction

changing the height which the crucible extended above the top of the upper inert diffusion layer. Assumptions used in this experimental design were:

1. The gaseous products of reaction do not react with the diffusion layer.
2. The effective diffusivity through the inert diffusion layer is equivalent to the effective diffusivity through the reactant bed.
3. Heat transferred to the reactants will vary as a function of the path length for thermal diffusion and thermal mass.
4. The rate of mass transfer through the porous solid bed will vary as a function of the path length for mass diffusion.
5. The rate of mass transfer through the boundary layer in the gas phase above the solid bed will vary as a function of the gas phase diffusion path length.

Table 1 summarizes the experimental design. A series of four base case experiments were run; labeled B12, B15, B13, and B14. In these four cases only the diffusion layer above the sample bed was varied thereby changing both the intra-bed diffusion path length and the thermal mass. Additional experiments B16 through B21 were designed to investigate specific deviations from the base case series. Experiment B16 had the same thermal mass as experiment B14 and the same diffusion path length as experiment B12. Run B17 was a duplicate of run B13 to test reproducibility. Experiment B18 used purge gas containing 21 percent, 0.21 atmosphere, CO. Experiments B19, B20, and B21 had identical intra-bed diffusion layer thickness as B12 with different gas phase diffusion path lengths. Temperatures and weights of the samples were continuously monitored and recorded.

Results and discussion

A simple set of three experiments were run to screen the observed reaction process for the influence of transport and kinetic effects. For each of these three experiments the gas flowrate and crucible cross-sectional area were held constant while the initial sample weight was varied. The observed reaction rates were significantly different such that the global rate of weight loss decreased as the sample mass was increased. Figure 2 illustrates the experimental results for these cases where an increase in sample mass was directly proportional to the thickness of the sample bed:

$$\text{sample mass} = IA\varrho \tag{6}$$

where I equals the depth of powder sample in the crucible, A equals the cross sectional area of the crucible which was constant, and ϱ equals the bulk density of powder sample which was also constant. Changing the sample mass in this way influenced the mass transfer within the sample bed and the gas phase product over-

Table 1 Experimental design to control factors influencing the observed rate of reaction

Run no.*	Sample wt. (mg)	Crucible height (cm)**	wt. of inert SiO_2 layers		Crucible wt.	Thermal mass of SiO_2	Total thermal	Gas comp.	Gas flow (SCCM)
			above sample	below sample					
Base case series									
B12	177	0	437.4	0.0	1700.5	437.4	2137.9	Ar	21.5
B15	176.8	0	757.1	0.0	2204.0	757.1	2961.1	Ar	21.5
B13	176.3	0	1193.7	0.0	2518.1	1193.7	3711.8	Ar	21.5
B14	174.2	0	2006.5	0.0	4769.9	2006.5	6776.4	Ar	21.5
Separation of thermal and bed diffusion effects									
B-6	175.2	0	442.8	1568.2	4810.7	2001.0	6821.7	Ar	21.5
Duplicate of run B13									
B17	173.4	0	1198.7	0.0	2740.0	1198.7	3938.7	Ar	21.5
Effect of CO over-pressure									
B18	173.9	0	1195.0	0.0	2737.9	1195.0	3932.9	21% CO	21.5
Effect of gas phase transport									
B19	176	1.72	442.1	0.0	4031.5	442.1	4473.6	AR	21.5
B21	175.9	0.95	429.2	0.0	3283.9	429.2	3713.1	AR	21.5
B20	177.1	0.46	433.2	0.0	2314.0	433.5	2747.5	AR	21.5

* Run numbers are consistent and taken from the more detailed publication reference number (1).

** Height that crucible extends above the top of the SiO_2 diffusion layer.

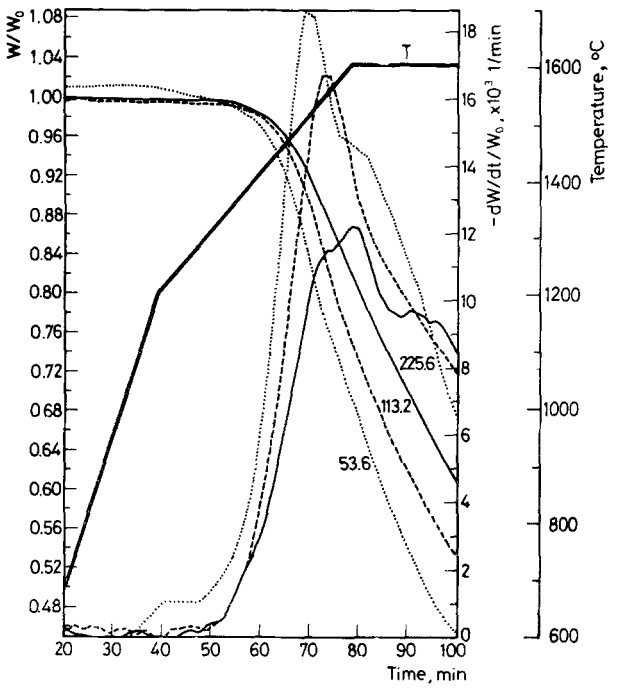

Fig. 2 The effect of sample mass on the reaction of carbon powder and silica powder; —— W/W_0 and $-dW/dt/W_0$ for W = 225.6 mg, – – – W_0 = 113.2 mg, . .–. . W_0 = 53.6 mg. Temperature profile: 30 deg/min to 1200 °C, 10 deg/min to 1600 °C

pressure which depends on the chemical reaction rate, amount of chemical reaction, and flowrate of purge gas. Heat transfer should not have been affected since the surface to volume ratio did not change. The rate of weight loss, and hence the rate of reaction, was found to be affected by the initial sample weight. Using this simple experimental design, however, it is virtually impossible to determine which phenomenological factors are responsible for the observed changes.

To clarify which rate controlling phenomena is dominant in the reaction process, a more detailed series of experiments were run using the design described above; illustrated by Fig. 1 and defined by Table 1. Figure 3 summarizes the results of a base case series. The four TGA curves generated have the common characteristic of two distinct stages. The first stage consists of initial rapid reaction during the non-isothermal segment which carries into the isothermal segment. The second stage is a constant rate period characterized by much lower rate of weight loss than the initial rapid rate stage and followed by decreasing reaction rates at high extents of reaction. The effect of changing the diffusion layer thickness and thermal mass was

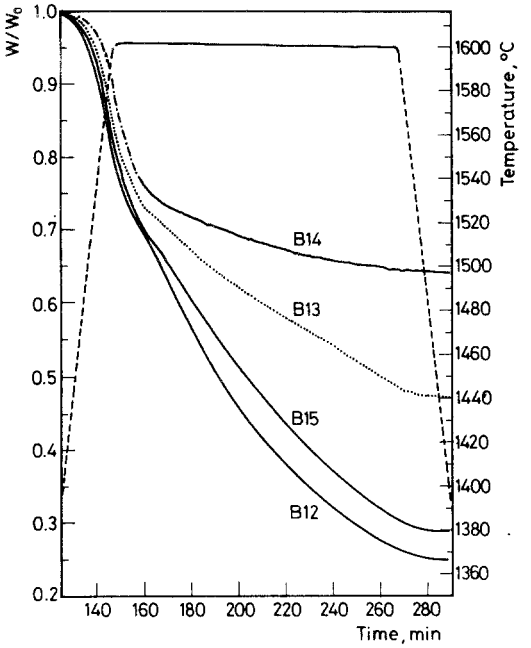

Fig. 3 The effect of bed diffusion and thermal mass on the reaction of carbon powder and silica powder samples when heated at 10 deg/min; W/W_0 —— Run B12, ... Run B13, . . _ . . Run B15, —.—. Run B14, – – – temperature profile

to shift the DTG of the rapid rate period towards higher temperatures leaving the observed maximum rate unchanged within the degree of reproducibility of the experiment. The observed constant rate during the second segment of reaction was decreased with increasing thermal mass and intra-bed diffusion layer thickness. Quantitatively there were two distinct processes being observed. This can be demonstrated by correlating the off-gas analysis for CO and the weight loss data. When compared, the derivative TG (DTG) and the derivative off-gas data for CO indicate that a distinct change in reaction stoichiometry occurs coincident with the abrupt change in reaction rate observed at the transition from the first to the second stage of reaction. Figures 4a and 4b illustrate the off-gas derivative as a function of run time plotted along with the integral TG and DTG data for run B16. A comparison of the off-gas derivative and DTG data revealed a change in stoichiometry characterized by the change in relative area below the derivative curves. Biernacki [1] has previously shown that this change is a result of a change in global reaction stoichiometries from formation of SiC via the two-step series of reactions (1) and (2) to SiO formation by reaction (3). This distinct separation of reaction stoichiometries makes it possible to analyze the two stages of reaction

independently. Results presented for run B16 are characteristic of all the experiments in this series. From this series alone, however, it was impossible to distinguish between the thermal, mass transfer, and chemical kinetic effects.

Further experimentation enabled thermal and mass transfer and kinetic effects to be characterized. Heat transfer at the temperatures of interest is less likely to be a rate controlling factor since heat transfer will occur by predominantly radiation. Comparison of experiments B12, B14 and B16 clearly identified the changes in observed reaction rate as being the result of mass transfer within the porous solid bed. Figure 5 illustrates that run B16 had identical observed reaction rates as compared to run B12 although the thermal mass was different. Both runs B16 and B12 had identical diffusion path lengths. When compared to run B14, which was thermally identical to B16 but had a different intra-bed diffusion layer thickness, a distinct difference was observed. It can safely be concluded from this experiment series that the observed rates of reaction under the specified conditions appear not

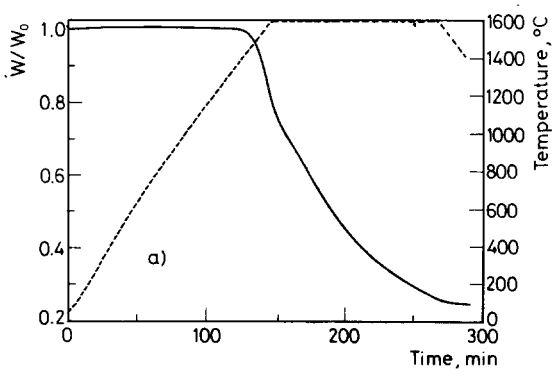

Fig. 4a TGA and temperature profile for Run B16; —— $\overline{W/W_0}$, ... temperature profile

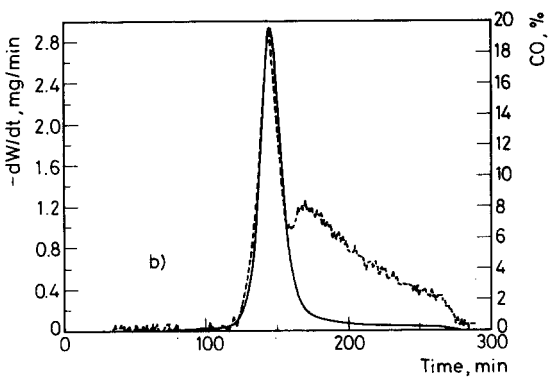

Fig. 4b Off-gas derivative and DTG for Run B16; —— % CO, – – – dW/dt

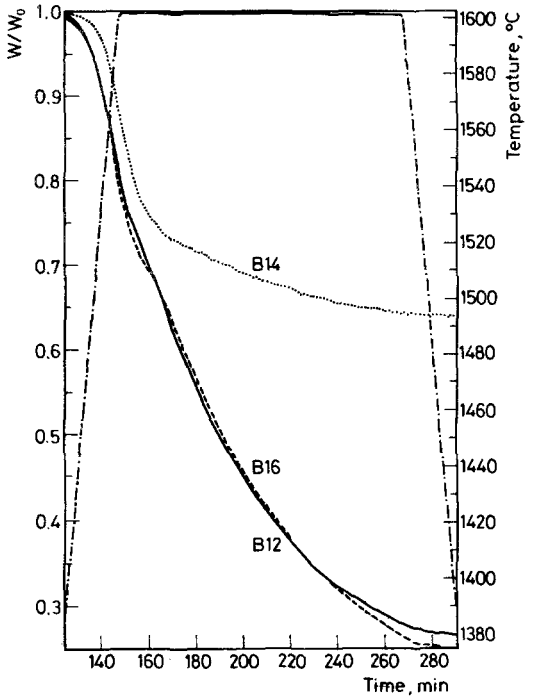

Fig. 5 Separation of thermal and bed diffusion effects; W/W_0 —— Run B12, ... Run B1 4, – – – Run B16, . . – . . temperature profile

to be influenced by heat transfer through the sample bed. In each of these experiments the gas phase transport conditions above the bed surface were not changed. Therefore, it can be concluded that the diffusion path length through the porous solid bed significantly influences the observed reaction rate. Thus, changes in the intra-bed diffusion path length, not heat transfer effects, are responsible for the differences noted in the base case series illustrated by Fig. 3. Although thermal transport is less likely to be a factor at these higher temperatures, it is prudent to demonstrate this experimentally. When studying systems at lower temperature this analysis may reveal important information relating the rate of reaction and heat transfer.

Additional experiments were designed to vary the gas phase transport conditions above the sample bed. Experiments B19, B20, and B21 had the identical intra-bed diffusion layer thickness, as experiment B12, however, the crucible height was extended above the surface of the exposed diffusion layer. This modification in the experiment provided a change in transport conditions above the sample bed with Fig. 6 illustrating the results of these four experiments. From this data it can be

seen that the second stage of reaction, e.g. that characterized by the reaction of SiO_2 with SiC via reaction (3), is moderately affected by changes in the gas phase transport conditions above the bed surface. For shallow crucibles, however, the effect was completely eliminated as shown by a comparison of experiments B12 and B20 which had crucible heights of zero and 0.45 cm respectively. The first stage of reaction, e.g. that characterized by the formation of SiC via the series path of reactions (1) and (2), was unaffected by these gas phase transport conditions in every case. Table 1 summarizes these and other results. From this series of experiments it can be concluded that the observed rate of reaction is not influenced by gas phase transport conditions above the bed when the crucible is shallow and gas flow above the bed surface is unrestricted.

Additional analysis of the data from runs B12 through B21 was done to see how strongly the reactions are influenced by intra-bed diffusion. The activation energy for the global rate process responsible for the first stage of reaction could be calculated. This first stage of reaction was carried out to near completion during the

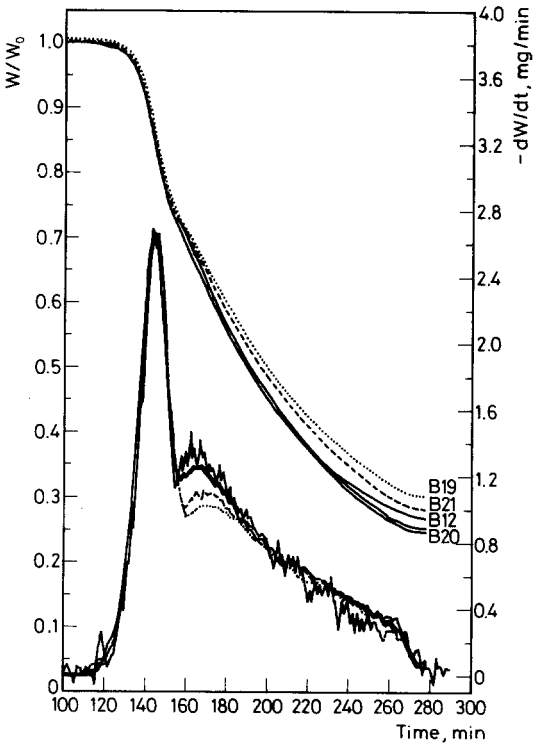

Fig. 6 Separation of bed diffusion and gas phase transport effects; W/W_0 and $-dW/dt$ for —— Run B12, ... Run B19, = = = Run B20, - - - Run B21

non-isothermal segment of the experiment; therefore activation energies could be computed for each run. In this analysis the global observed activation energy was calculated using an Arrhenius plot and assuming zero order kinetics since the literature suggested that this reaction can be approximated as a zero order phenomenon (at least for low extent of reaction). Table 2 lists the calculated zero order rate parameters, including the pre-exponential constant, Arrhenius activation energy, and the correlation coefficient of the linear fit.

Table 2 Zero order rate analysis for experiments designed to control factors influencing the observed rate of reaction

Run no.	Weight loss range $W_1/W_0 - W_2/W_0$	Temp. $T_1 - T_2$	$\ln(A_0)$	$\varrho_{\ln(A_0)}$	E_a, kcal/gmole	σ_{E_a}	Correlation coefficient
B12	1 − 0.81	1400–1600	16.27	1.09	74.81	3.82	0.941
B15	1 − 0.81'	1400–1600	20.57	0.86	90.58	3.03	0.973
B13	1 − 0.85	1400–1600	25.22	0.92	107.75	3.25	0.979
B14	1 − 0.899	1400–1600	26.68	0.99	114.64	3.5	0.978
B16	1 − 0.81	1400–1600	17.17	0.96	77.83	3.4	0.956
B18	1 − 0.93	1400–1600	37.23	1.55	153.37	5.45	0.985
B19	1 − 0.84	1400–1600	17.97	1.34	81.12	4.72	0.961
B21	1 − 0.84	1400–1600	17.48	1.20	79.24	4.22	0.967
B20	1 − 0.82	1400–1600	16.23	1.43	74.58	5.03	0.948

Consistent with data reported in the literature for this reaction, the data shown here indicates that the activation energy is roughly 90 kcal/gmole[5], although, values between 70 kcal/gmole[4] and 122 kcal/gmole[2] have been reported. In addition the global rate process can be empirically expressed as a zero order kinetic process with a high degree of statistical confidence, although this by no means indicates that the process is in reality controlled by a zero order reaction mechanism. In spite of the fact that the activation energy is high enough to suggest that the process is kinetically controlled, it is clear from the previous discussion that intra-bed diffusion does influence the reaction rate. Activation energies for gas phase diffusion controlled processes at 1200 to 1600° should be on the order of ten to 20 kcal/gmole. The large difference between the observed activation energy and that expected for diffusion control suggests that diffusion does not control the rate of reaction for the first stage of reaction. It is clear, however, that the rate of reaction is influenced by changes in the transport conditions. This conclusion is demonstrated by the observed shift in TGA curves with respect to time and temperature as a function of diffusion layer thickness as illustrated by the base case

series shown on Fig. 3 and is mathematically expressed by variations in the calculated empirical zero order kinetic constants.

For every case the second stage of reaction occurred during the isothermal segment of the experiment. This stage of reaction was characterized by the formation of SiO via reaction (3) which occurred at a roughly constant rate for low extent of reaction. This constant rate, however, was found to be dependent upon the intra-bed diffusion layer thickness as illustrated by Fig. 5. Constant rates of reaction observed in this context can indicate that the reaction is either zero-order kinetic dependent or that it is controlled by diffusion; however, the fact that the observed constant rate is a function of the diffusion layer thickness suggests that the reaction may be controlled by intra-bed diffusion rather than by zero-order chemical kinetics. The observation that the constant rate period rapidly turns into diminishing rate behaviour also indicates that the reaction is not controlled by zero order chemical kinetics.

In order to determine how strongly the observed rate of reaction during the second stage is influenced by mass transport effects, the rate data was evaluated using a traditional diffusion controlled model. Under isothermal conditions diffusion controlled behaviour follows Fick's first law:

$$\Phi_i = D_{e,i}\frac{dC_i}{dx}, \tag{7}$$

where Φ_i equals the mass flux of species i through the intra-bed diffusion layer, $D_{e,j}$ equals the effective intra-bed diffusivity for species i, and dC_i/dx equals the concentration gradient of species i through the diffusion layer. The concentration gradient, dC_i/dx, is given by

$$\frac{dC_i}{dx} = \frac{1}{x}(C_{eq,i} - C_{s,i}) \tag{8}$$

where x equals the intra-bed diffusion layer thickness, $C_{eq,i}$ equals the equilibrium concentration of species i at the bottom of the diffusion layer, and $C_{s,i}$ equals the concentration of species i at the surface of the diffusion layer. Upon substitution the flux can be expressed as:

$$\Phi_i = (C_{eq,i} - C_{s,i})\frac{D_{e,j}}{x} \tag{9}$$

A simple test for diffusion control in these experiments is to plot Φ_i *vs.* $1/x$. At constant temperature the resulting line should be straight with slope $(C_{eq,j} - C_{s,i})D_{e,i}$. A non-linearity would not, however, rule out diffusion influence in this case since deviations from linearity could indicate combined kinetic-diffusion

control. The instantaneous slope of the Φ_i *vs.* $1/x$ plot, however, must be equal to or less than the theoretical value of $(C_{eq,i} - C_{s,i})D_{e,\ i}$ since the reaction cannot proceed faster than the maximum rate dictated by diffusion control.

Figure 7 illustrates Φ_{co} *vs.* $1/x$ for the constant rate period of experiments B12 through B18 and experiment B20. Experiments B19 and B21 were omitted since they were influenced by gas phase film diffusion. The rate was estimated by

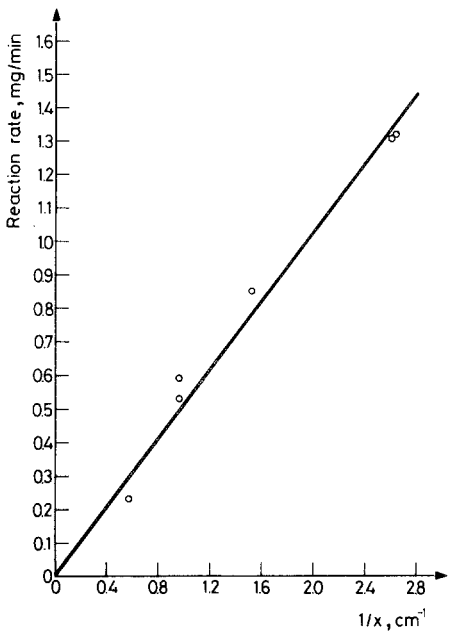

Fig. 7 Reaction rate *vs.* the inverse of diffusion path length for the second stage of reaction, $2SiO_2 + SiC \rightarrow 3SiO + CO$; O measured data, ——— curve fit $0.516 * (1/x) - 1.242 * 10^{-5}$

determining the slope of the constant weight loss period of the integral TG curve for each run. The bulk density of the SiO_2 powder and the crucible inner diameter were used to compute the thickness (x) of the diffusion layer. Constant rate data and diffusion path-length thickness are summarized in Table 3. From Fig. 7 it can be seen that the constant rate data falls on a straight line with an effective diffusivity for intra-bed diffusion of CO[16] computed as:

$$D_{e,\text{obs,CO}} = 0.7 \text{ cm}^2/\text{sec}$$

The effective diffusivity was also estimated from first principles as:

$$D_{e,\text{est,CO}} = 4.35 \text{ cm}^2/\text{sec}$$

The lower value computed from experimental data indicates that the reaction is

most likely not completely controlled by intra-bed diffusion. The difference of less than one order of magnitude does suggest, however, that the reaction rate is near the diffusion limit. The observed dependence of reaction rate on the extent of reaction, as illustrated by the decreasing rate of reaction with increasing extent of reaction, suggests that the process is not strictly controlled by diffusion for higher extents of reaction. This result combined with the strong observed dependence on the diffusion path length for low extent of reaction verifies that the reaction is controlled by combined diffusion and kinetic phenomena with the dependence changing as a function of the extent of reaction.

Table 3 Constant rate data summary for various experiments

Run no.	Diffusion layer thickness $1/x$ (cm^{-1})	Reaction rate (mg/min)
B12	2.63	1.32
B16	2.6	1.31
B15	1.52	0.85
B13	0.96	0.53
B17	0.96	0.59
B14	0.57	0.23

The present study has found the rate of the SiO_2/C reaction to be influenced, but not controlled, by mass transfer diffusion within the reactant bed. However, nothing has been said of the effect of CO over-pressure on the reaction rate. The effect of diffusion layer thickness, shifting of the weight loss curve towards higher temperature and longer time as a function of diffusion layer thickness, does suggest that the kinetics have an inverse dependence upon product over-pressure. The effect of increased diffusion path length is to increase the local product over-pressure within the reactant bed thereby slowing the reaction. If indeed the product over-pressure, e.g. the CO over-pressure, has this effect, then artificially increasing the CO over-pressure should have a similar result as increasing the diffusion path length. Run B18 was an identical duplication of Run B13 in as far as the intra-bed diffusion path length, total gas flowrate, initial sample mass, and gas phase transport conditions were concerned. This run differed from B13 in that the feed gas contained roughly 21 percent CO as compared to zero CO for run B13. Figure 8 illustrates the results of run B18 as compared to run B13 and B14. Run B18 was found to be similar to run B14 which had a thicker diffusion layer. As compared to run B13, run B18 displayed the same type of shift with respect to temperature (or time) as did runs having a thicker diffusion layer. Similarly, the effect of CO over-

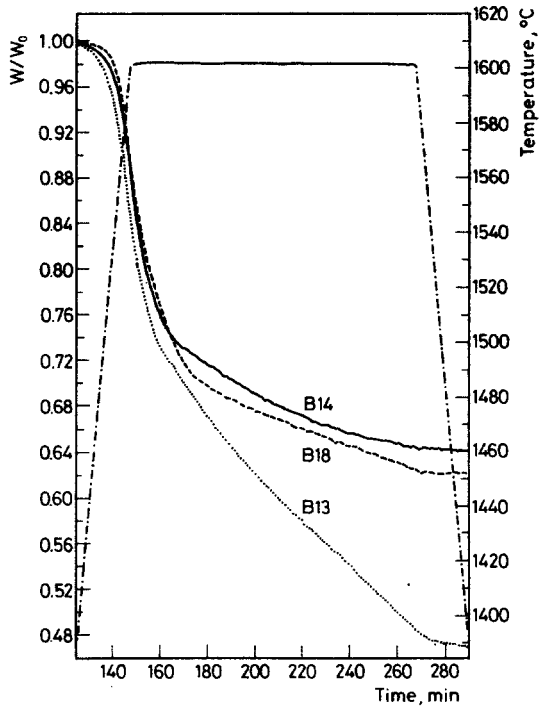

Fig. 8 The effect of carbon monoxide over-pressure; .... W/W_0 Run B13, ——— Run B14, . – . – Run B18 (P_{co} = 0.21 atm), .. – .. temperature profile

pressure on the second stage of reaction was the same as found by increasing the diffusion layer thickness. These results demonstrate that the effect of intra-bed diffusion is to slow the reaction rate via CO over-pressure dependence.

Conclusions

As in previous work, the $SiO_2 + C$ reaction was found to proceed via a reaction path in which a large change in stoichiometry can be identified by observing that the ratio of the weight loss integral to the integrated amount of CO changes as a function of time. This change is abrupt and, hence, two stages of reaction can be postulated and treated independently. Both stages of reaction have been found to be influenced, but not controlled, by diffusion mass transfer within the reacting bed of solids. This conclusion applies particularly to the second stage of reaction in which SiO_2 and SiC react to form SiO gas.

References

1 J. J. Biernacki, "Formation of Silicon Monoxide and Application to the Growth of Vapor-Liquid-Solid Silicon Carbide Whiskers," Doctoral Dissertation, Fenn College of Engineering, Cleveland State University, Cleveland, Ohio, 1987, p. 378.

2 N. Klinger, E. L. Strauss and K. L. Kosmarek, J. Amer. Cer. Soc., 49 (1966) 369.

3 J.-G. Lee and I. B. Cutler, Cer. Bul., 65 (1975) 195.

4 F. Viscomi and L. Himmel, J. Metals, (1978) 21.

5 J. B. Henderson and M. R. Tant, Polymer Composites, 4 (1983) 233.

6 Fisher Scientific S–153 240 mesh floated silica (α-quartz).

7 R. T. Vanderbilt Company, Inc., Termax carbon powder.

8 H. E. Kissinger, J. Res. Nat. Bureau Stand., 57 (1956) 217.

9 E. S. Freeman and B. Carroll, J. Phys. Chem., 62 (1957) 394.

10 A. W. Coats and J. P. Redfern, Nature, 201 (1964) 68.

11 H. L. Friedman, J. Pol. Sci. C, 6 (1965) 183.

12 T. Ozawa, Bull. Chem. Soc. Japan, 38 (1965) 1881.

13 J. H. Sharp and S. A. Wentworth, Anal. Chem., 41 (1969) 2060.

14 J. H. Flynn, Organ. Plastics Chem., 44 (1981) 657.

15 J. P. Elder, J. Thermal Anal., 30 (1985) 657.

16 Details of this calculation are summarized in appendix VIII of reference 1.

Zusammenfassung — Mittels Thermogravimetrie wurde die Reaktionskinetik der Reaktion von kristallinem Siliziumdioxid und Kohlenstoffpulver im Molverhältnis 1 : 1 untersucht. Die kinetischen Angaben wurden mittels einfachen kinetischen und Stofftransportmodellen ausgewertet. Zu einer adäquaten Beschreibung der gesamten Reaktionserscheinung kann ein Zweischrittereaktionsmechanismus bestehend aus drei stöchiometrischen Reaktionen benutzt werden. Sowohl der erste als auch der zweite Reaktionsschritt wird durch diffusiven Stofftransport innerhalb des Reaktionsbettes beeinflußt.

Резюме — С помощью термогравиметрического анализа изучена кинетика реакции кристаллической двуокиси кремния и порошкообразного углерода, взятые в молярном соотношении 1 : 1. Результаты данных кинетики были оценены с помощью простой кинетической модели и масс-переноса. Двухстадийный реакционный механизм, состоящий из трех стехиометрических реакций, может быть адекватно использован для описания глобального реакционного явления. Установлено, что обе стадии реакции затрагиваются диффузионным массопереносом в пределах реакционного слоя твердых тел.